

# THREE DIMENSIONAL FLAME PROPAGATION ABOVE LIQUID FUEL POOLS

By Jinsheng Cai, Feng Liu, and William A.  
Sirignano

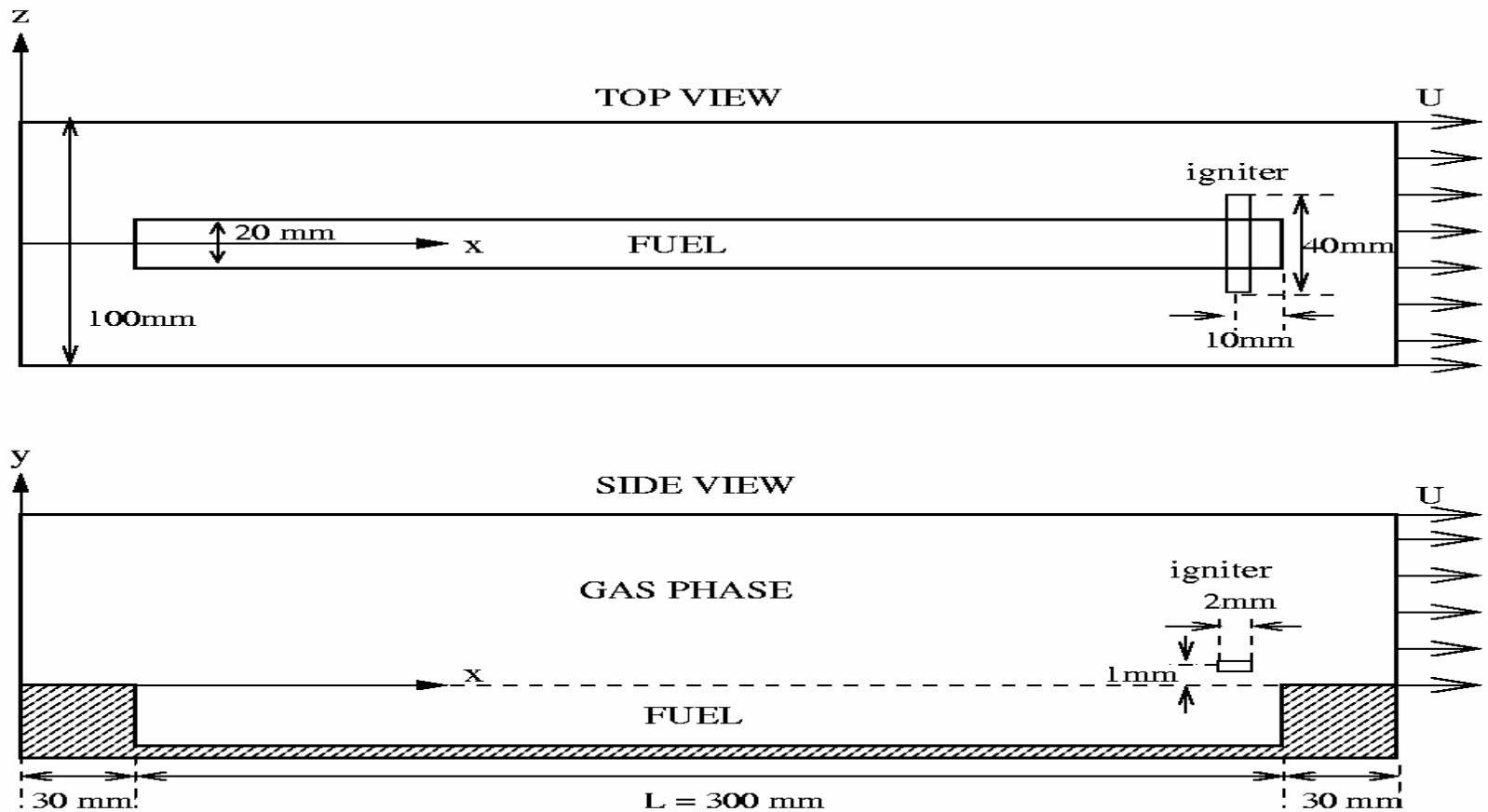
Mechanical and Aerospace Engineering  
University of California, Irvine

Supported by NASA Microgravity Program and  
Coordinated with NASA Glenn experimental  
work of H.D. Ross and F.J. Miller

# OBJECTIVES

- Examine 3-D effects for ignition and flame spread above a finite-width liquid-fuel pool. Determine pool-edge effects, flame curvature, lateral air and liquid motion.
- Determine flame speed, domains and frequency of pulsation, domains of uniform spread, flammability limits, and nature and size of recirculation zone.
- Analyze the influences of initial pool temperature, opposed-flow forced velocity, temperature-dependent surface tension, gas buoyancy, and liquid buoyancy.
- Guide and interpret drop-tower and sounding-rocket experiments of H. Ross and F. Miller of NASA Glenn.

# CONFIGURATION



3-D Liquid Fuel Pool in wind tunnel floor.  
Igniter modelled as a hot gas pocket with a linear temperature increase to  $1700$  K in  $0.01$ s.

# ASSUMPTIONS & CONDITIONS

- Unsteady, three-dimensional Newtonian flow.
- Laminar, viscous, multicomponent, reacting gas flow.
- Laminar, viscous, single-component, incompressible, vaporizing-liquid flow.
- Fourier heat conduction and Fickian mass diffusion.
- Variable properties.
- One-step chemical kinetics for alcohol fuel.
- Linear relationship between surface tension coefficient and surface temperature.
- Symmetry about the central vertical plane.
- Controlled air mass flow.
- A vaporized fuel layer develops over the fuel before the igniter is activated. The layer extends over the pool edge.

# DIFFUSION MODELS

- **Old Diffusion Model**

$$D_j = \frac{\mu}{\rho Sc} \quad j = 1, \dots, N$$

where  $\mu$  viscosity,  $\rho$  density,  $Sc$  Schmidt number,  $N$  number of species.

- **New Diffusion Model**

$$D_j = \frac{1 - Y_j}{\sum_{i \neq j}^N X_i / D_{ij}}$$

where  $D_{ij}$  is the binary diffusion coefficients

$$D_{ij} = \frac{0.00266T^{3/2}}{PM^{1/2}\sigma_{i,j}\Omega_D}$$

$$M_{ij} = \frac{2M_i M_j}{M_i + M_j} \quad \sigma_{ij} = \frac{\sigma_i + \sigma_j}{2}$$

$\Omega_D$  is a function of  $kT/\varepsilon$ ,  $M$  is molecular mass of species.  $\varepsilon$  and  $\sigma$  as the characteristic Lennard-Jones energy and length, respectively.

# NUMERICAL METHOD

- The numerical method uses the SIMPLE algorithm modified for second-order accuracy and to include an approximate factorization method to perform sub-iterations within each implicit time step.
- Only half of the wind tunnel is considered due to symmetry.
- A non-uniform mesh clustered grid points in the flame region is used.
- The grid lines are redistributed to concentrate in the flame region every time the flame front has moved 1 mm.
- Linear interpolation is used to map each dependent variable from the old to the new grid.

# CASES INVESTIGATED

**3D, 0-g, Hot Tunnel Floor (Insulated)**

**3D, 1-g, Hot Tunnel Floor (Insulated)**

**3D, 0-g, Cold Tunnel Floor (Heat Sink)**

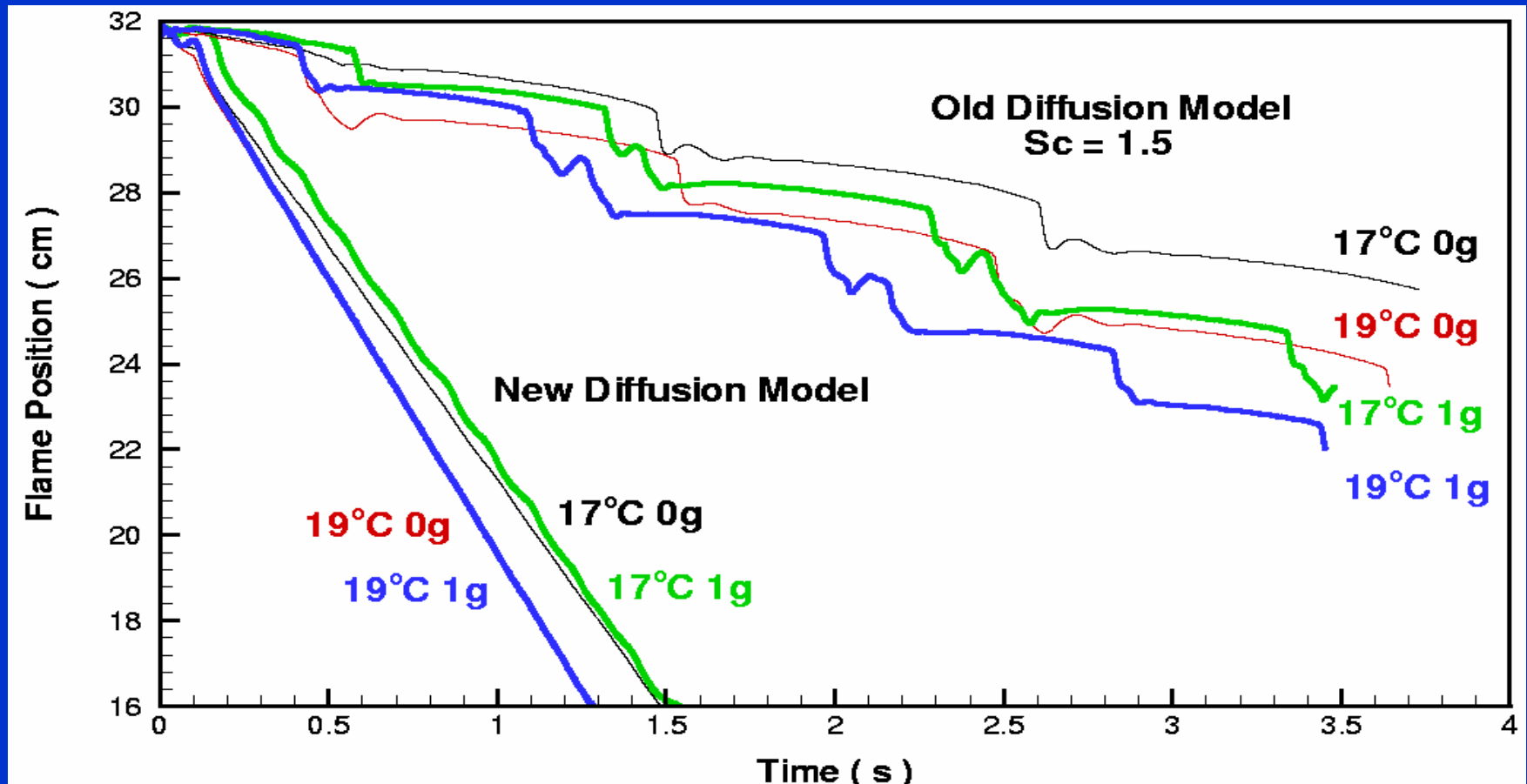
**3D, 1-g, Cold Tunnel Floor (Heat Sink)**

**2D, 0-g**

**2D, 1-g**

**Other Parameters: Propanol Fuel, Opposed  
air velocity = 30cm/s; Pool depth = 2mm;  
Initial Fuel Temperature = 11 to 19°C.**

# EFFECT OF DIFFUSION MODEL

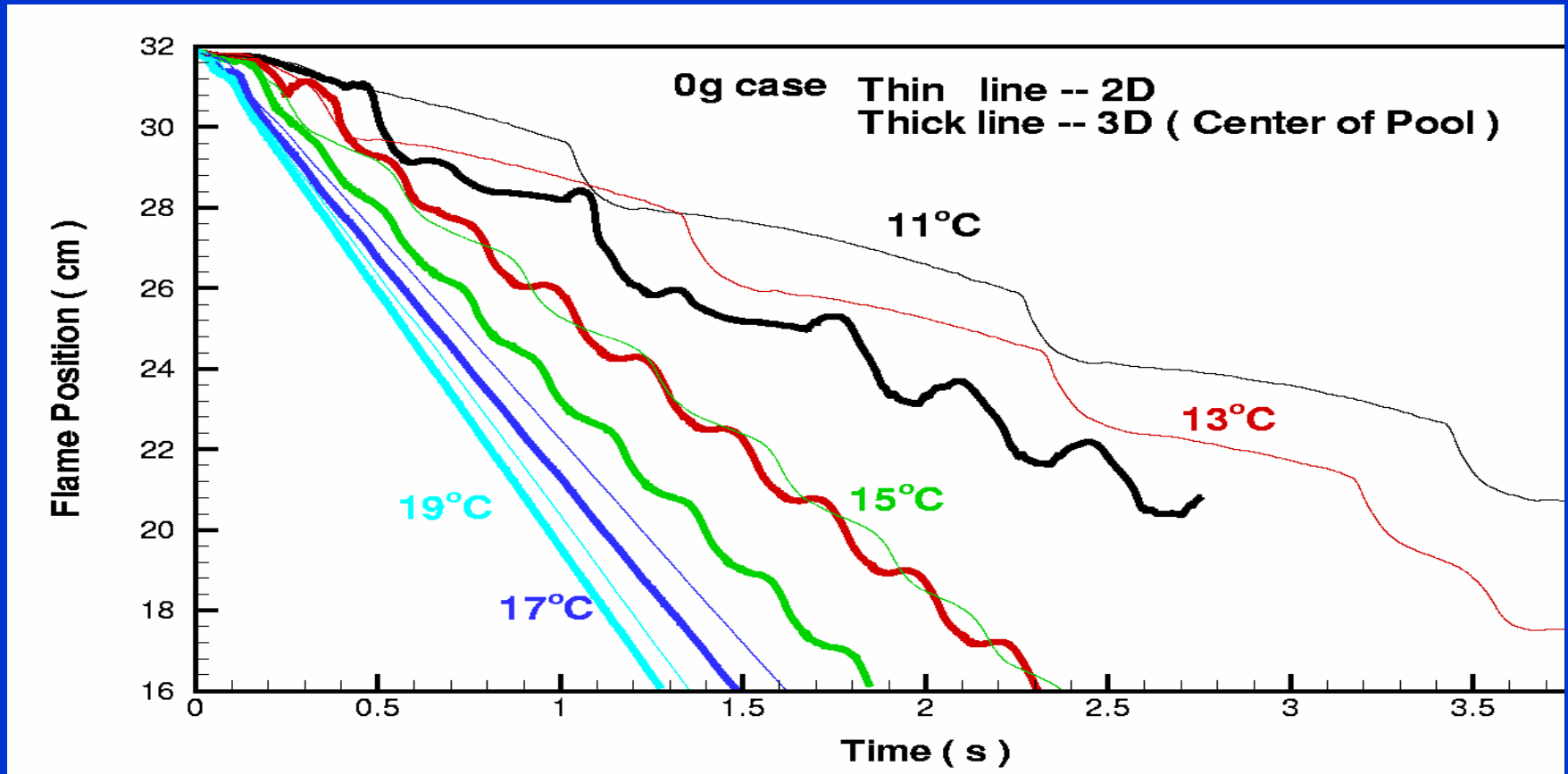


30 cm/s opposed flow. Flame speed and frequency increase with pool temperature. Pulsations occur at both 1-g and 0-g. Fast oxygen diffusion accounts for increased flame speed.



# 3D VS. 2D COMPARISON

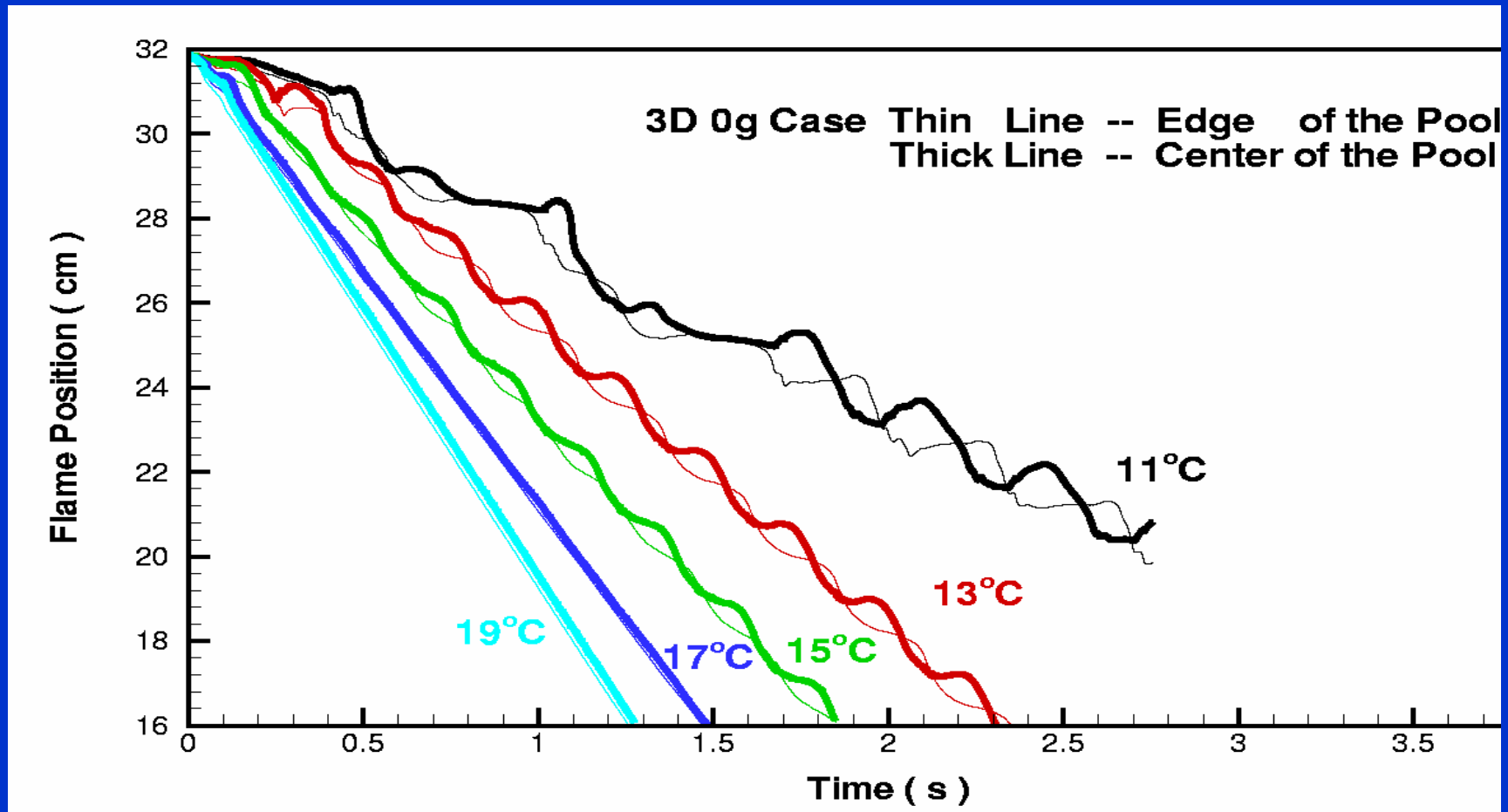
## Hot Tunnel Floor , 0-g, 30cm/s



Flame speed and frequency increase with pool temperature.

# FLAME POSITION VS. TIME

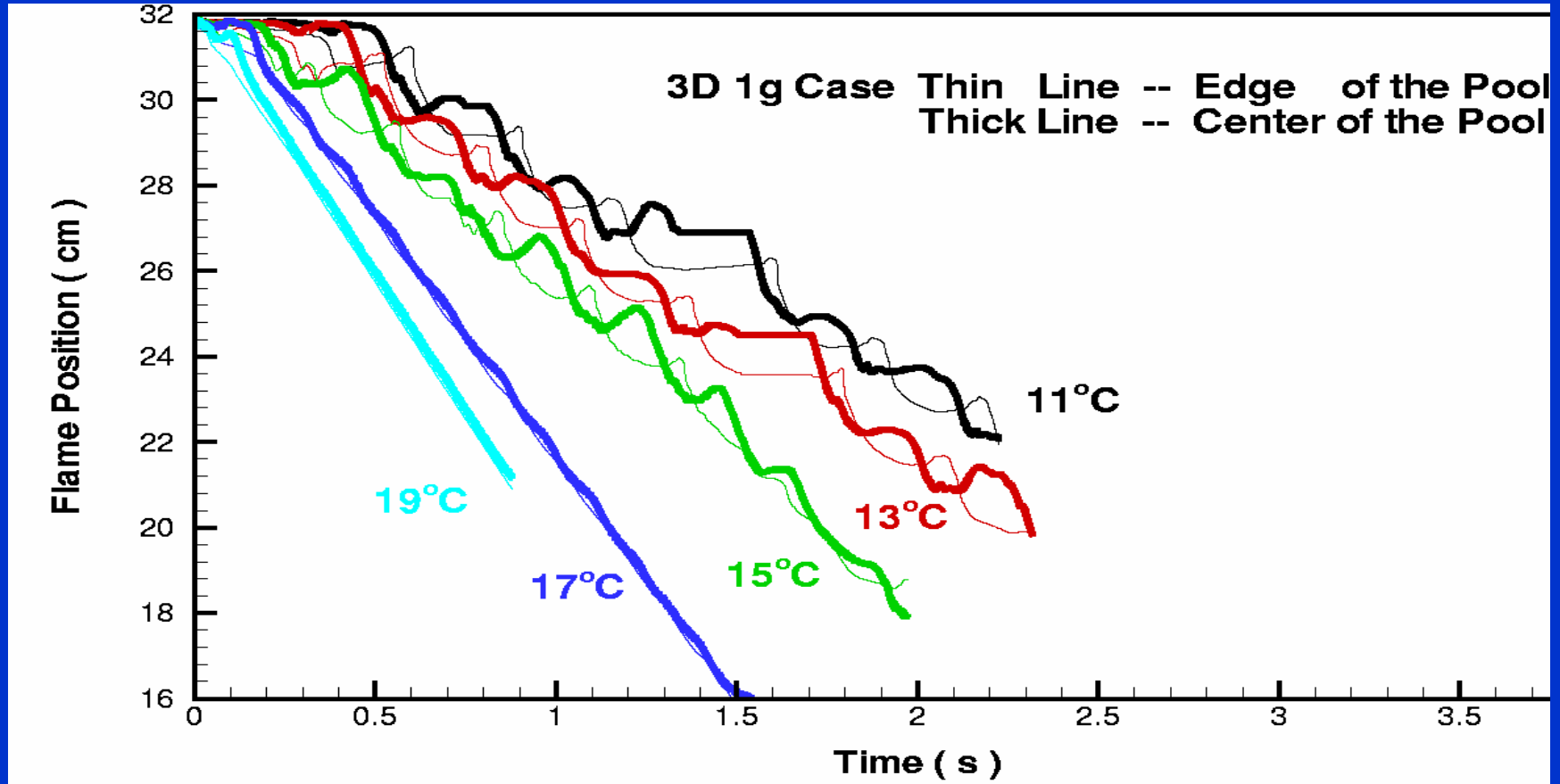
Hot Tunnel Floor, 0-g, 30cm/s



Flame speed and frequency increase with pool temperature.

# FLAME POSITION VS. TIME

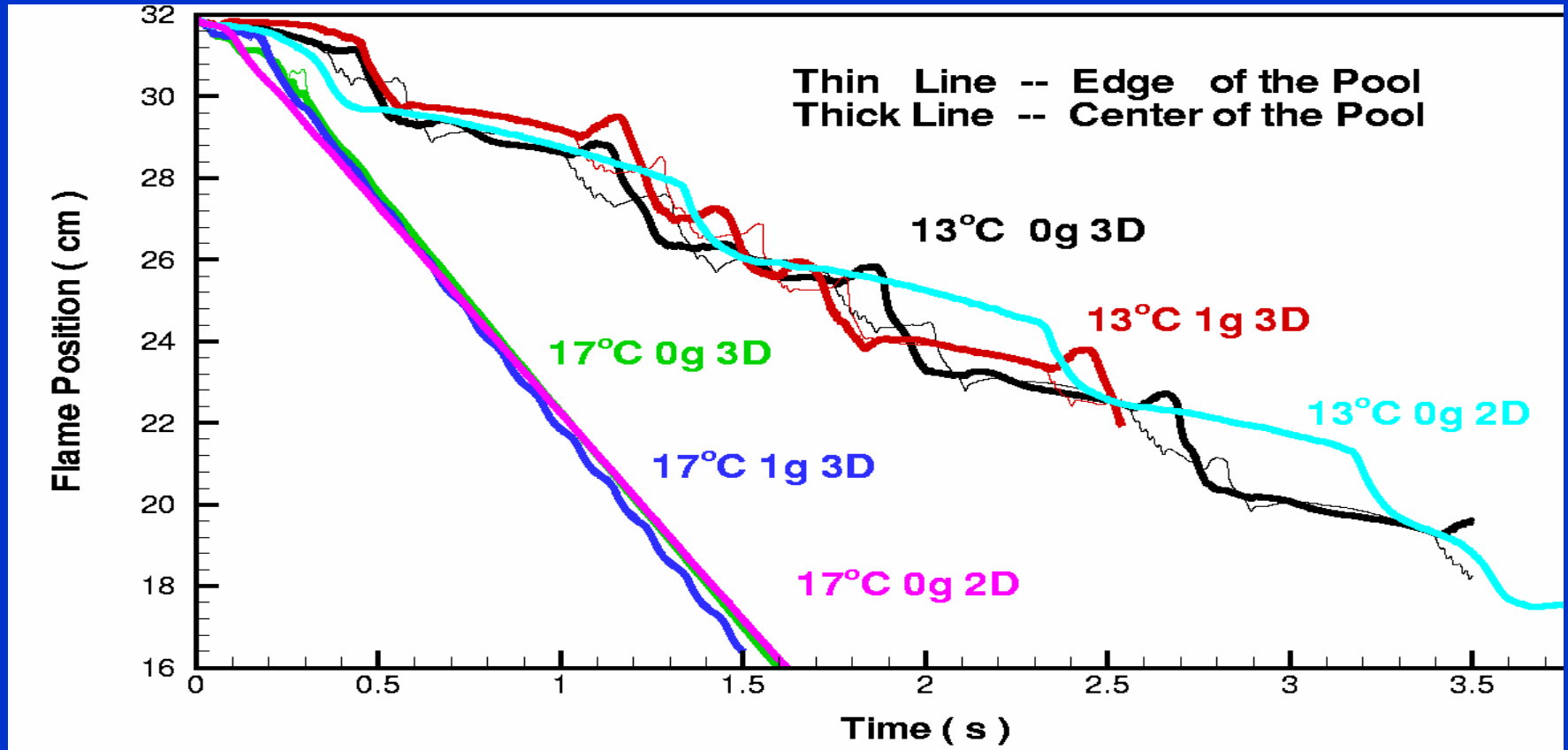
## Hot Tunnel Floor, 1-g, 30cm/s



Flame speed and frequency increase with pool temperature. Pulsations occur at both 1-g and 0-g.

# FLAME POSITION VS. TIME

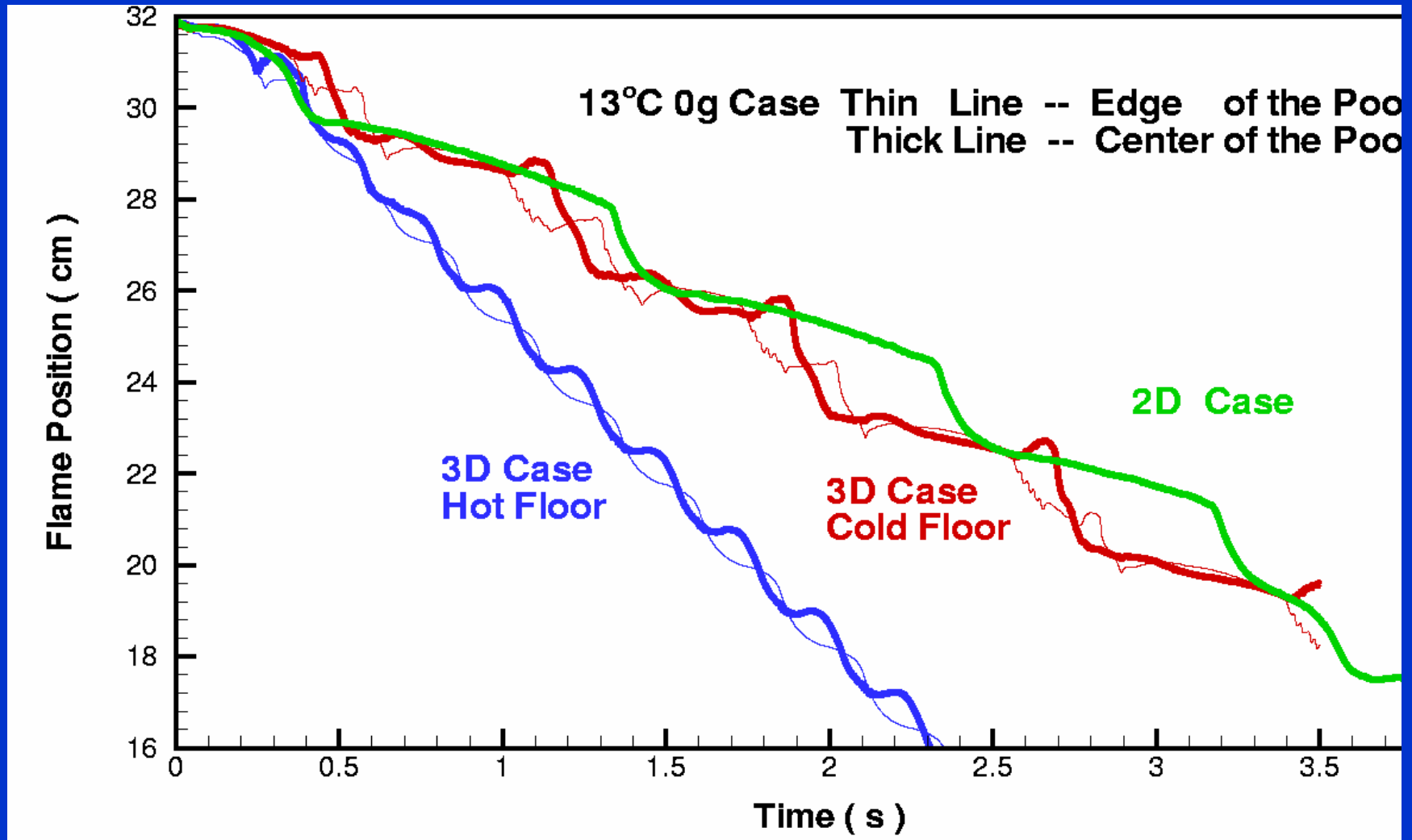
## Cold Tunnel Floor, 0-g and 1-g



30 cm/s opposed flow. Flame speed and frequency increase with pool temperature. Pulsations occur at both 1-g and 0-g.

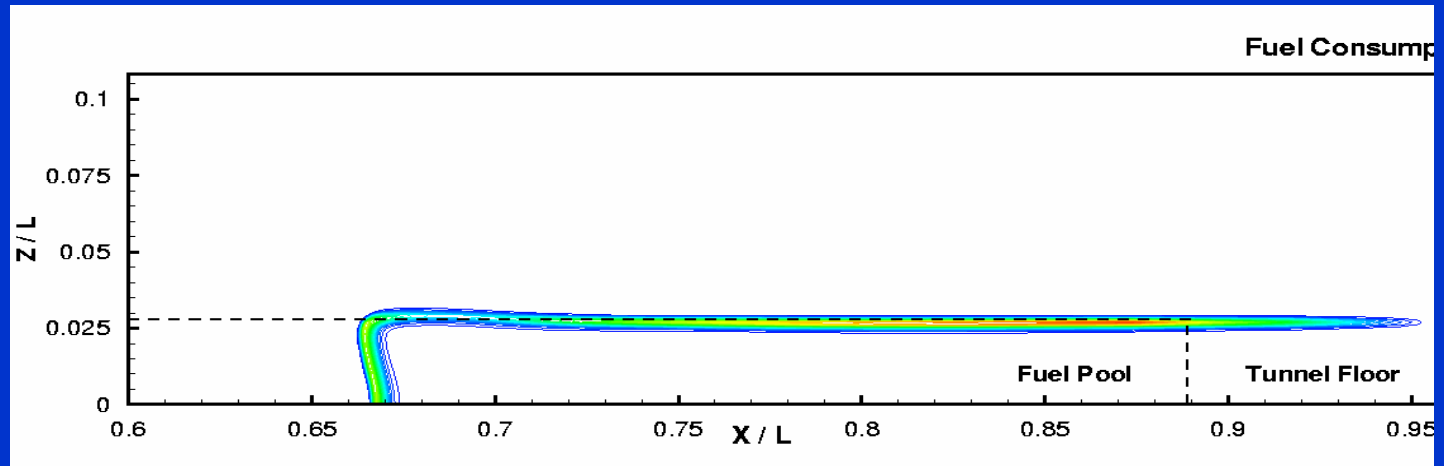
# FLAME POSITION VS. TIME

## Hot Floor, Cold Floor, and 2D

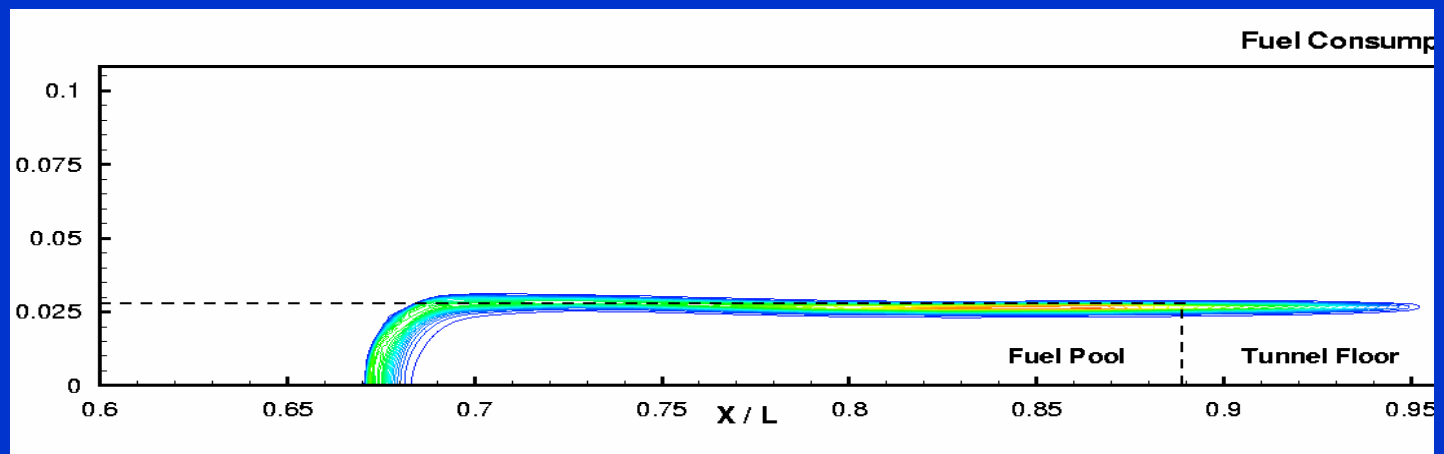


# Top View – Fuel Consumption Rate

Slow  
phase,  
 $t=2s$



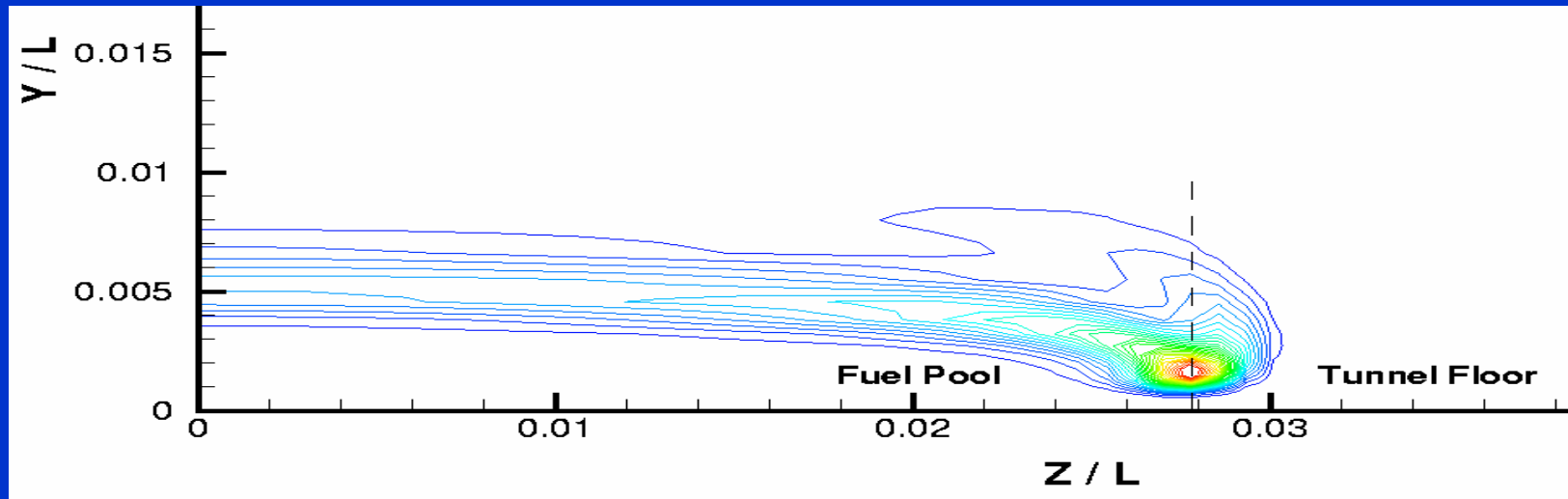
Fast  
phase,  
 $t=1.8s$



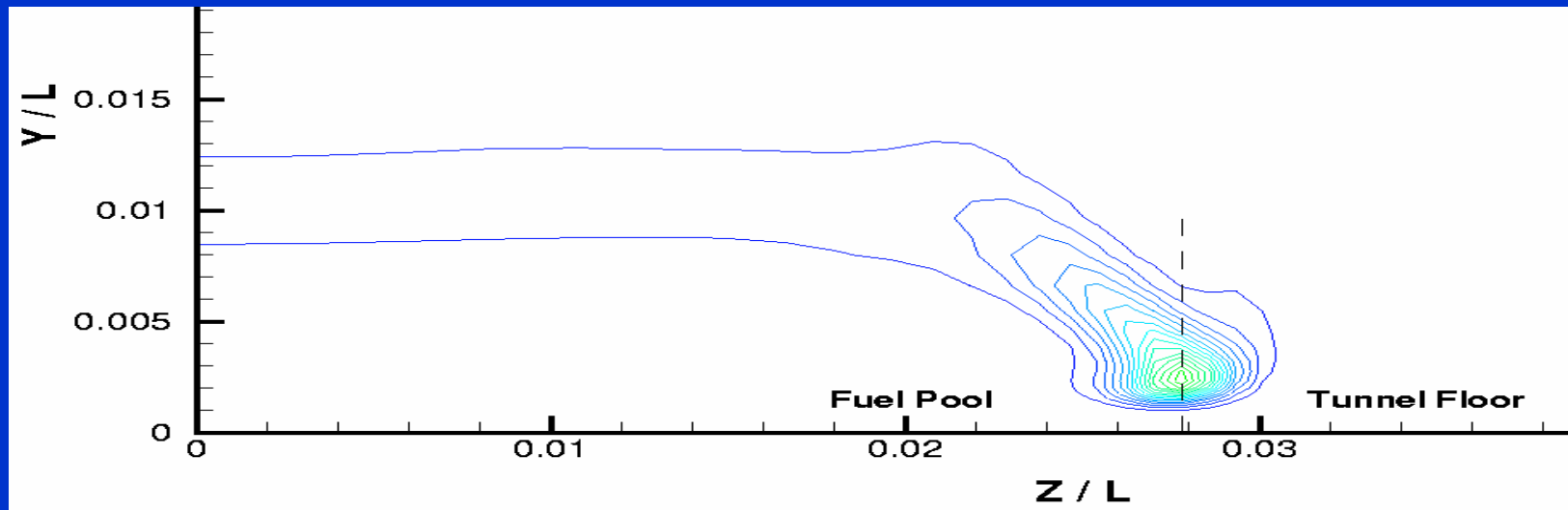
13 °C, pulsating case, 1-g,  $y=1mm$ . Cold Tunnel Floor. Flame tails lie along pool edge.

# Cross View – Fuel Consumption Rate

$x/L$   
 $=.69$

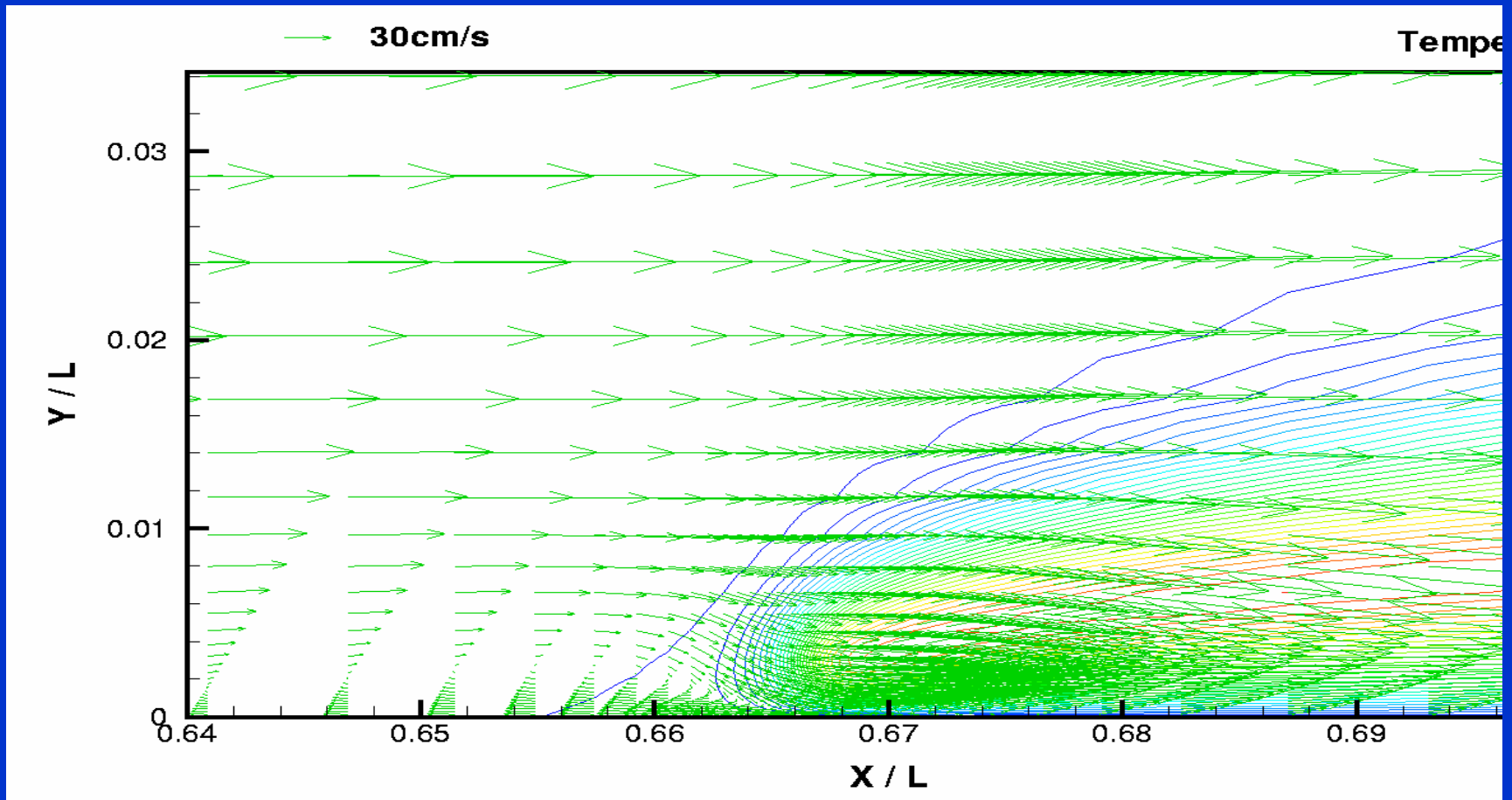


$x/L$   
 $=.75$



13 °C, pulsating case, 1-g,  $t=1.8$ s. Cold tunnel floor.

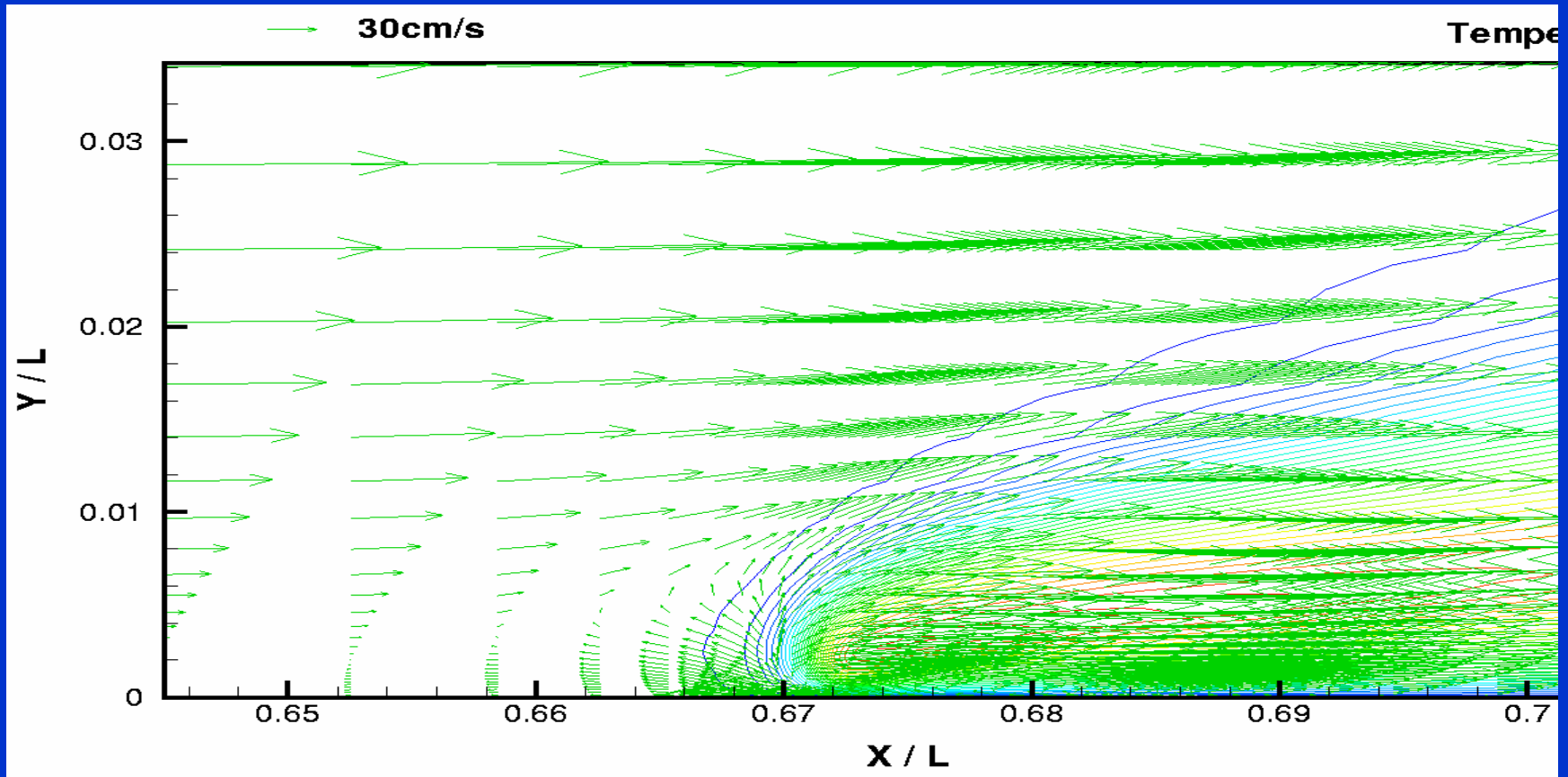
# Temperature Contours & Velocity Vectors – Slow Flame Phase



1g,  $t=2.0\text{s}$ ,  $z=0$ . Recirculation zone forms allowing fuel vapor accumulation.

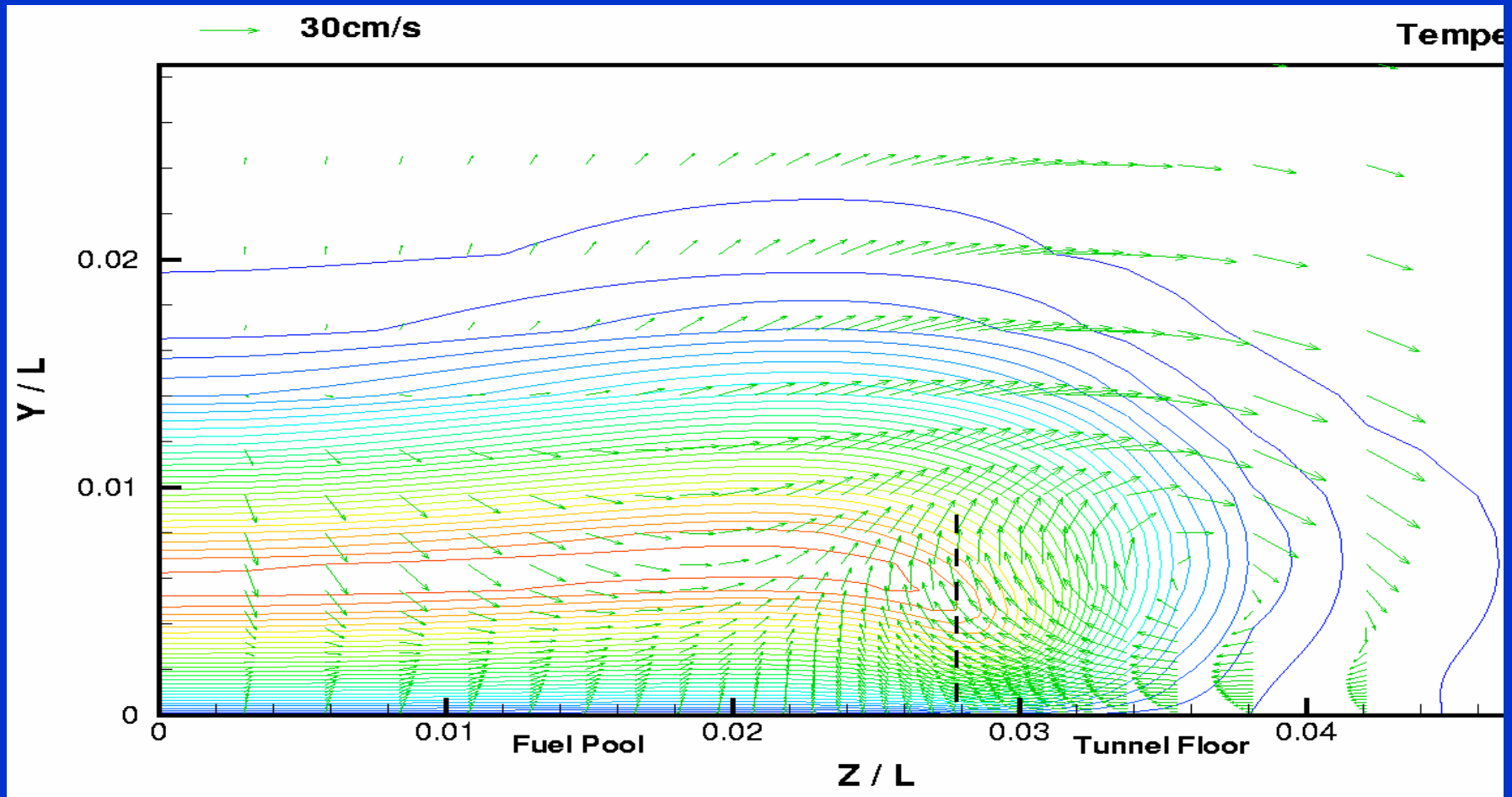


# Temperature Contours & Velocity Vectors – Fast Flame Phase



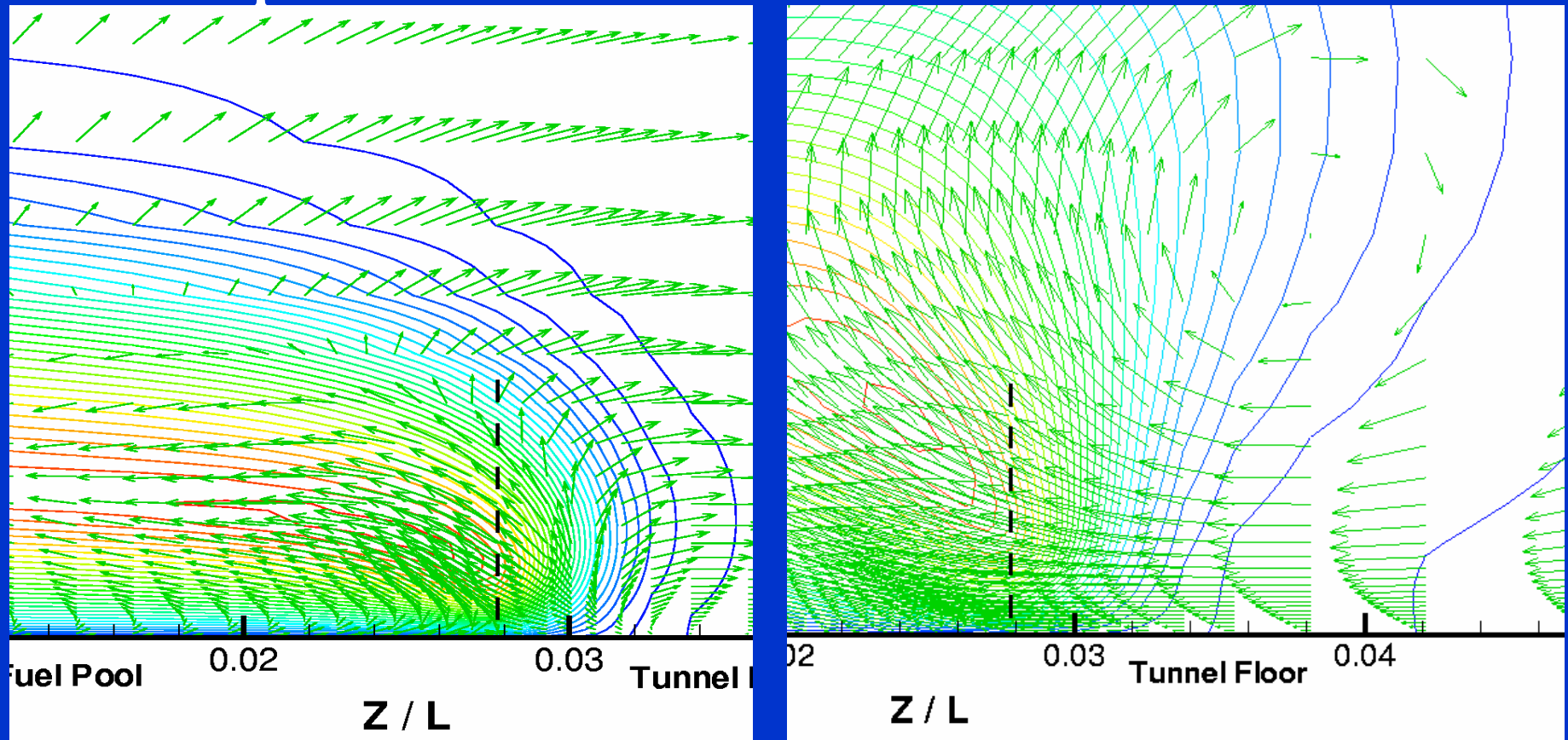
1g,  $t=1.8\text{s}$ ,  $z=0$ . Less recirculation,  
more hot gas expansion.

# Cross View - Velocity Vectors & Temperature Contours – Slow Phase



13°C, 1g,  $t=2s$ . Cold floor.  $x/L=0.68$ , recirculation.

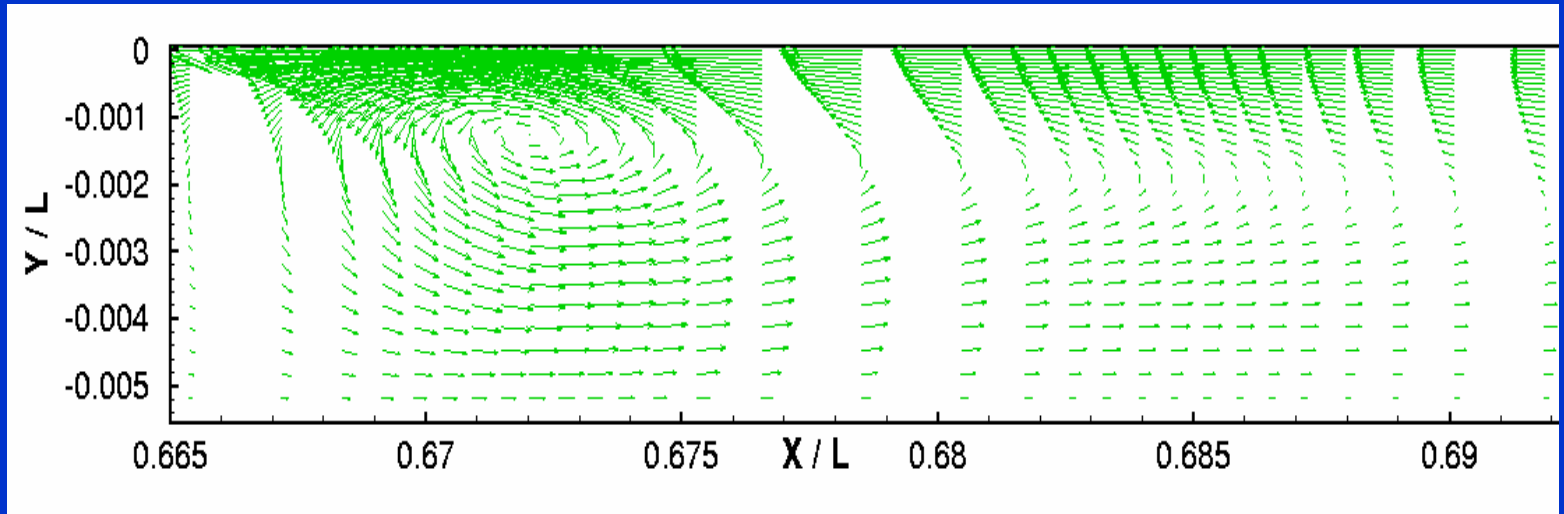
# Cross View - Velocity Vectors & Temperature Contours – Fast Phase



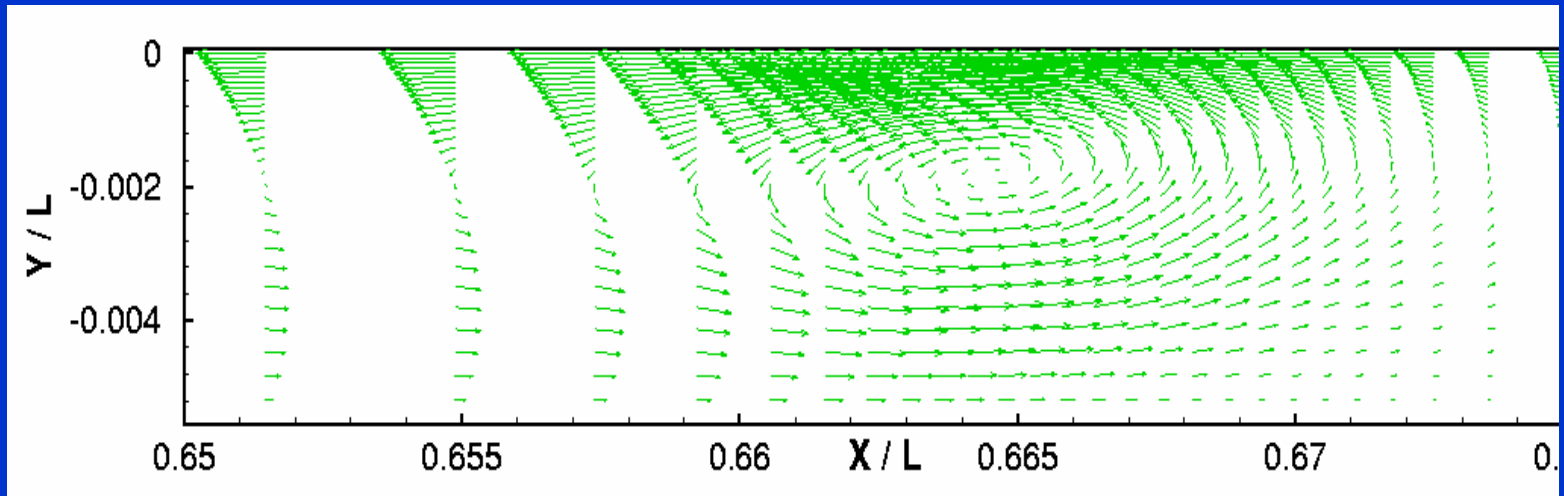
13°C, 1g,  $t=1.8s$ . Cold Floor.  $x/L=0.69$ ; expansion near flame front.  $x/L=.75$ , recirculation.

# Liquid Velocity

$t=1.8\text{s}$ ,  
fast  
phase

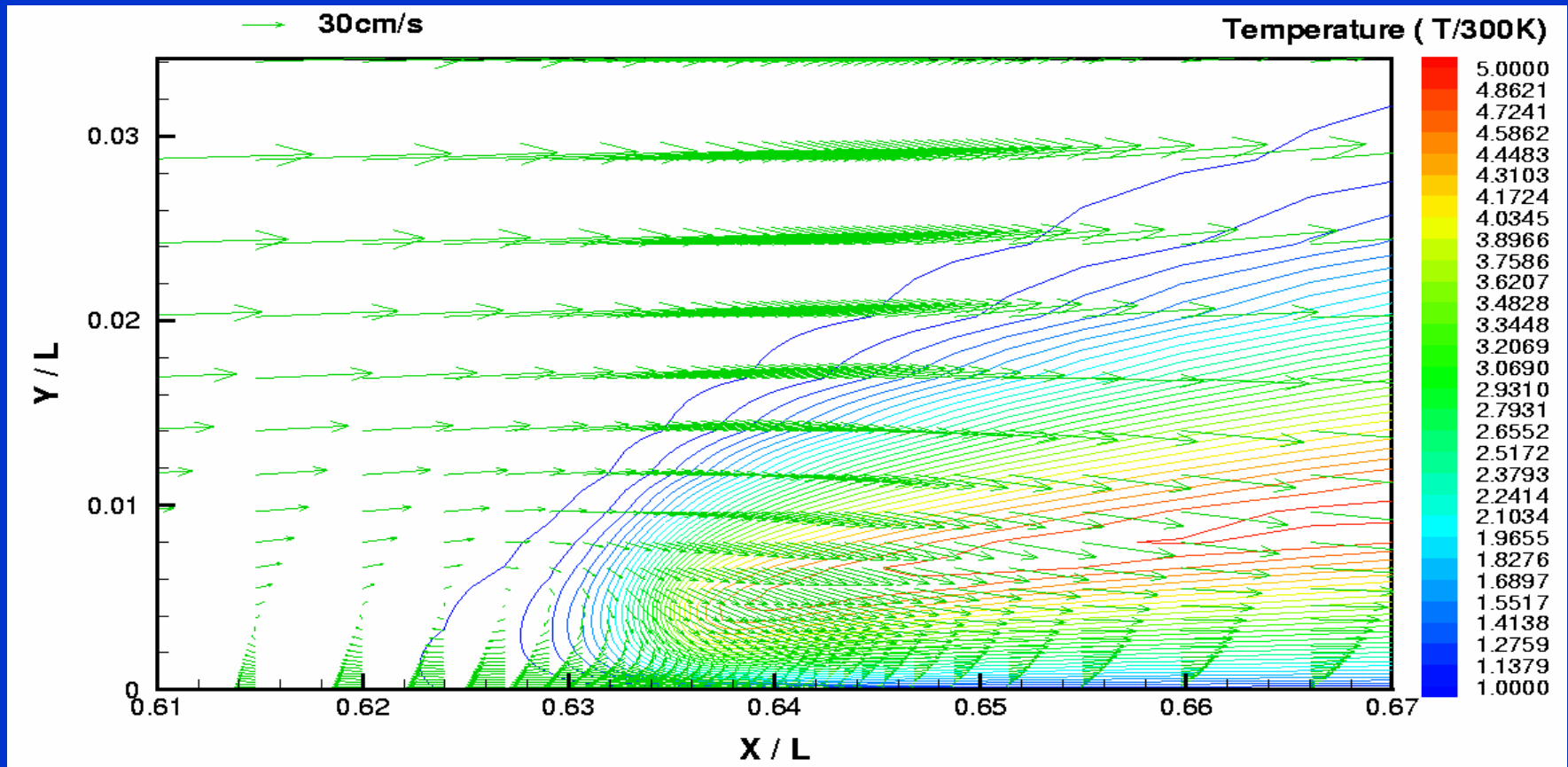


$t=2\text{s}$ ,  
slow  
phase



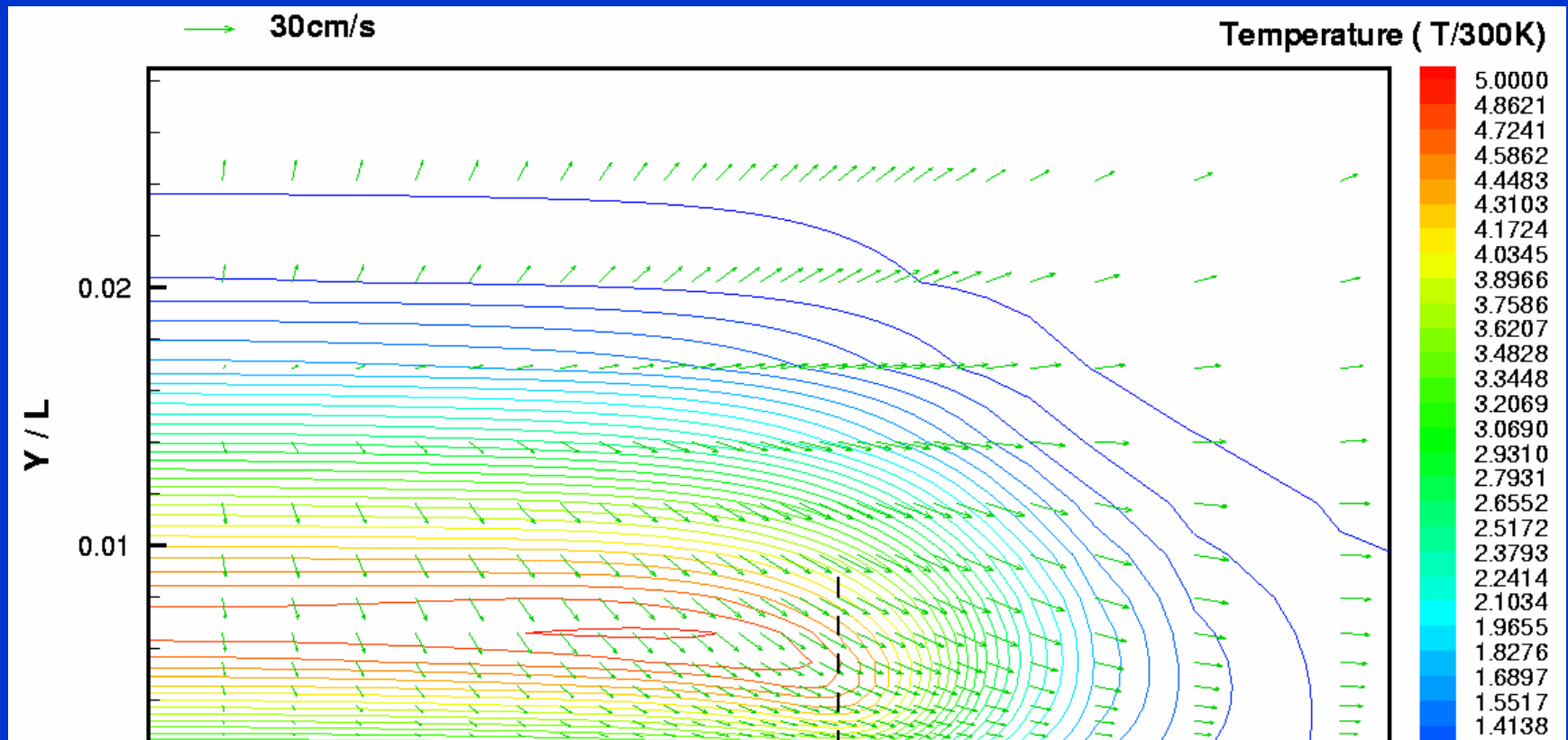
$13^\circ\text{C}$ ,  $1\text{g}$ ,  $t=1.8\text{s}$ . Cold floor. Surface tension plus buoyancy causes recirculation.

# Velocity & Temperature in Symmetry Plane



13°C, 0-g,  $t=2.3s$ , slow phase. Forced convection together with surface tension causes recirculation.

# Cross View - Velocity Vectors & Temperature Contours – Slow Phase



13°C, 0g, t=2.3s. Cold floor. x/L= 0.65.  
No side recirculation without buoyancy.

# CONCLUSIONS

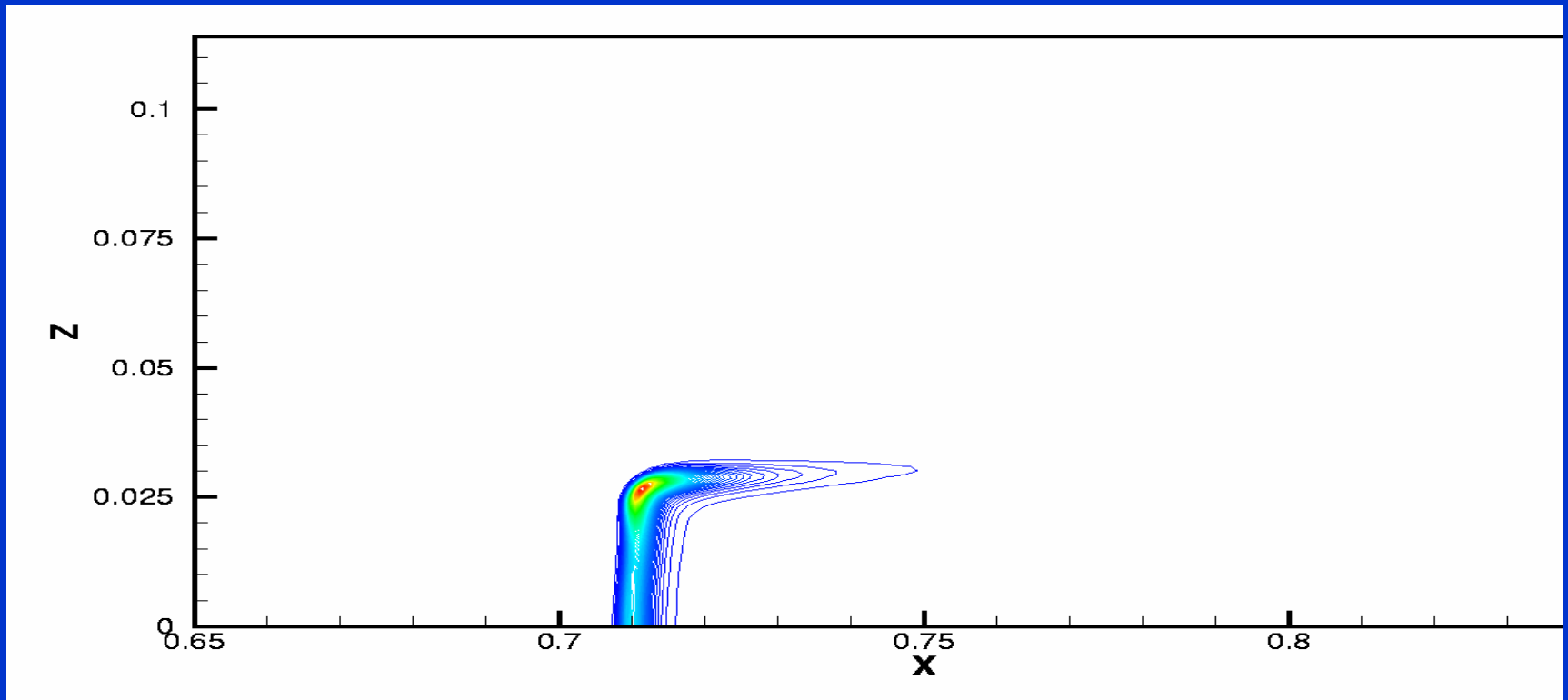
- Pulsations are found at both 0-g and 1-g with forced convection.
- Recirculation zone is key to mechanism for pulsation. Fuel vapor concentration increases during slow phase. Flammability limits are extended.
- Flame speed and pulsation frequency increase with initial fuel temperature.
- Improved diffusion model predicts faster propagation and uniform-rate spread / pulsating spread boundary moves to lower initial temperature.

# CONCLUSIONS (continued)

- Three-dimensional spread rate exceeds two-dimensional spread rate due to increased influx of oxygen.
- Increase in side heat losses reduces pulsating flame spread rate but has minor effect on uniform spread rates
- Flame front curves around pool edge extending along and setting over the pool edge.
- In 1-g case, buoyancy causes side vortices to form in pulsating spread.

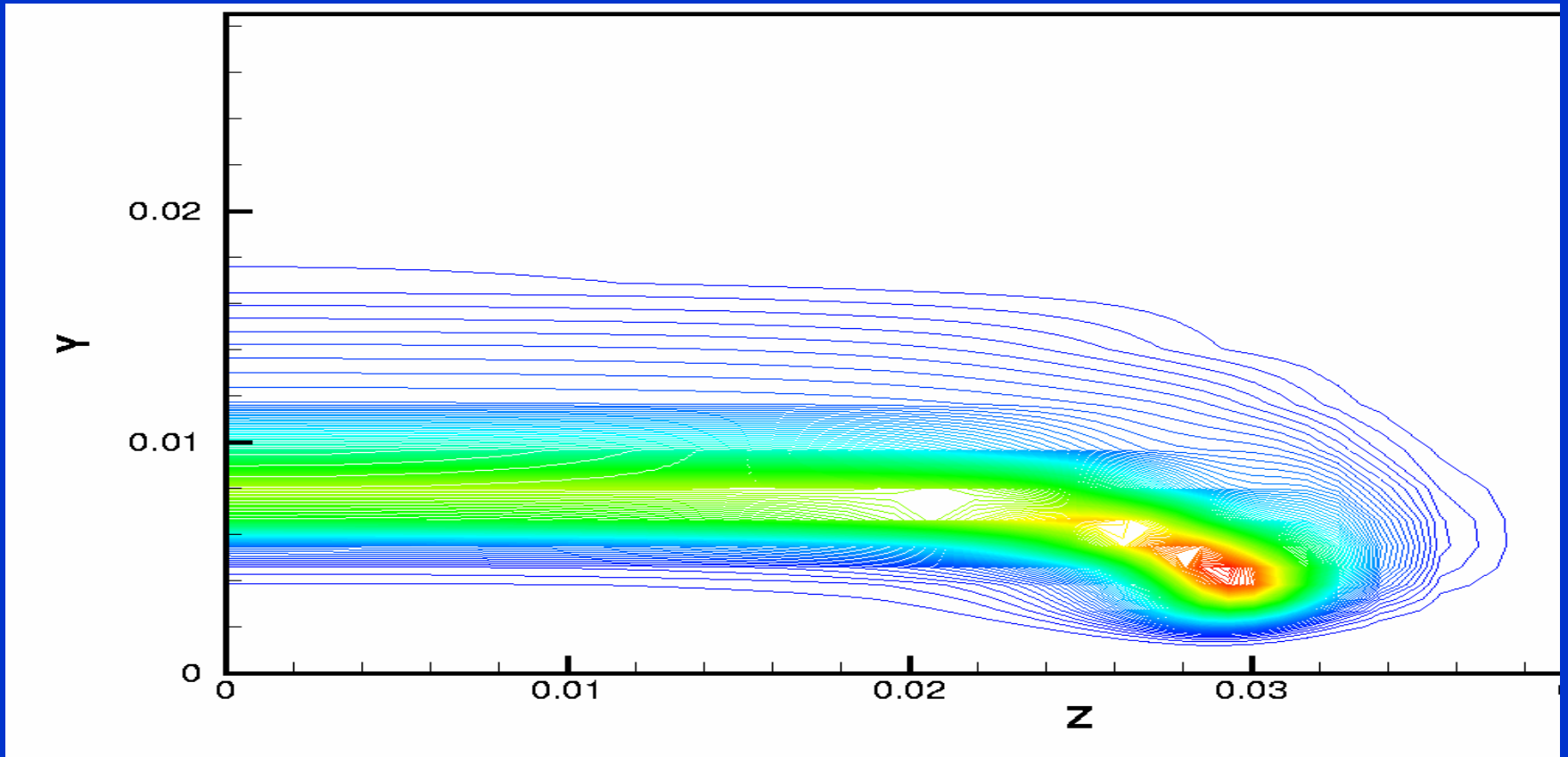


# Top View – Fuel Consumption Rate



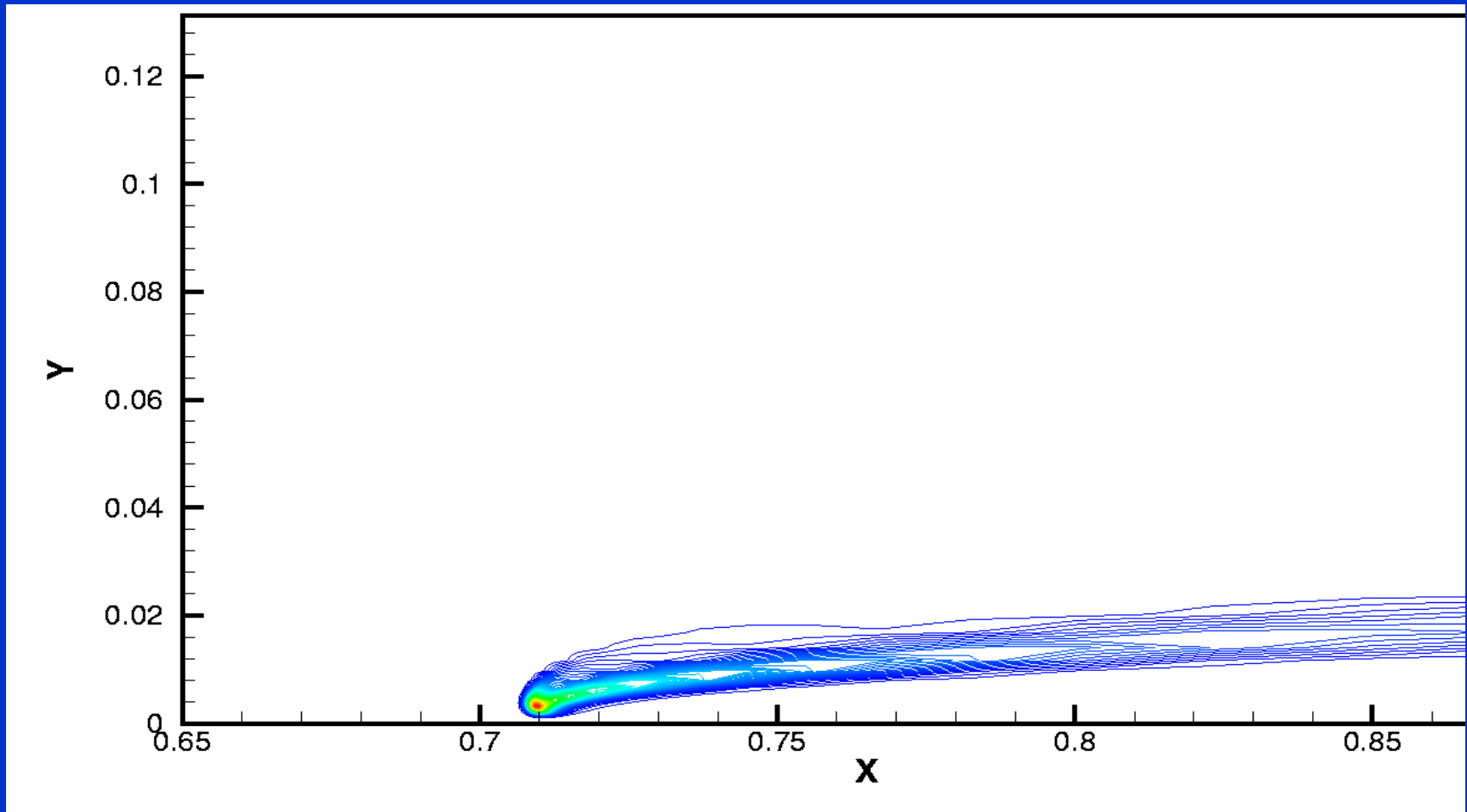
13 °C, pulsating case, 0-g,  $t=1.74s$ ,  $y=1mm$ . Cold Tunnel Floor. Flame tails along pool edge are short.

# Cross View, Behind Flame – Fuel Consumption Rate



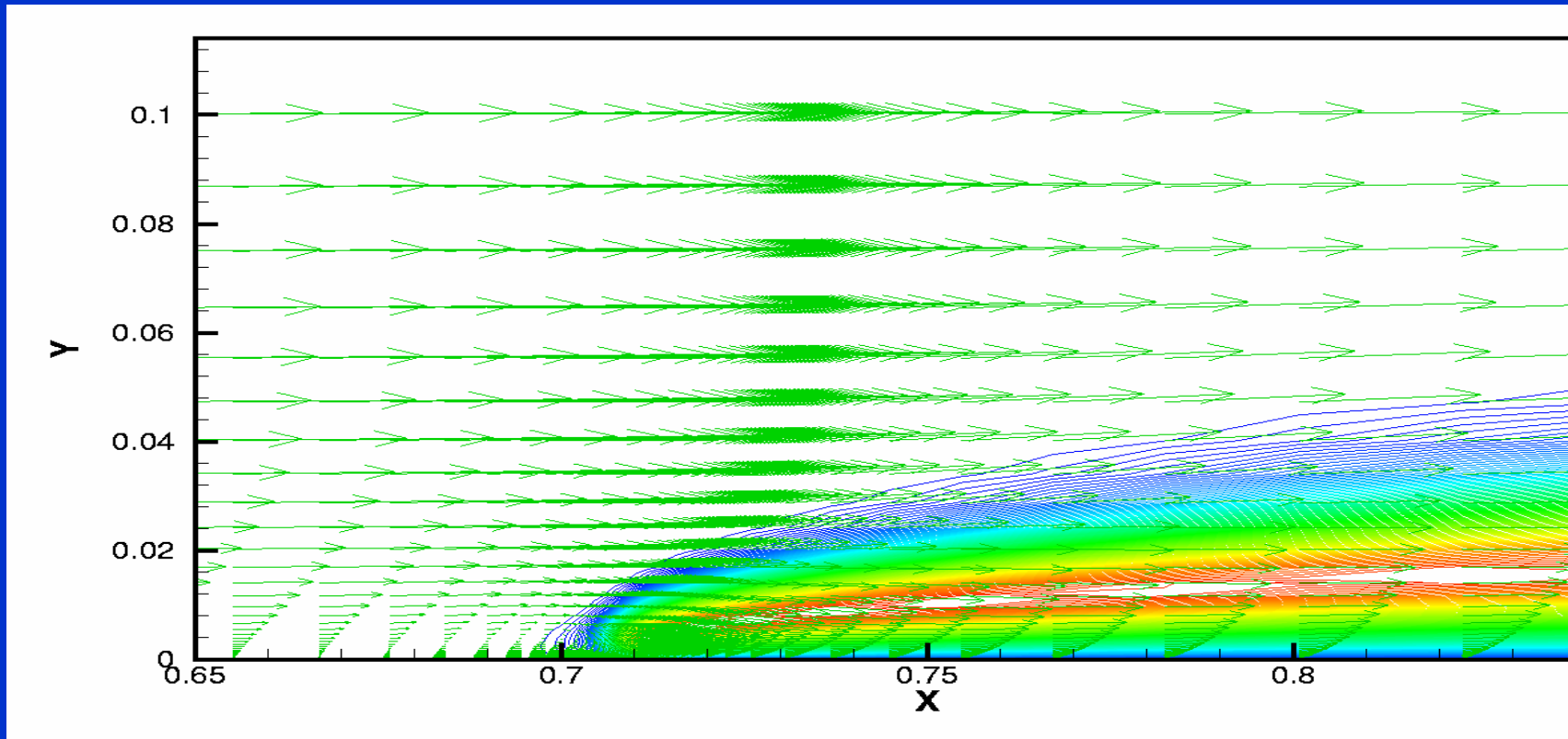
13 °C, pulsating case, 0-g,  $t=1.74\text{s}$ ,  $x/L=.73$ .  
Cold Tunnel Floor.

# Fuel Consumption Rate in Symmetry Plane



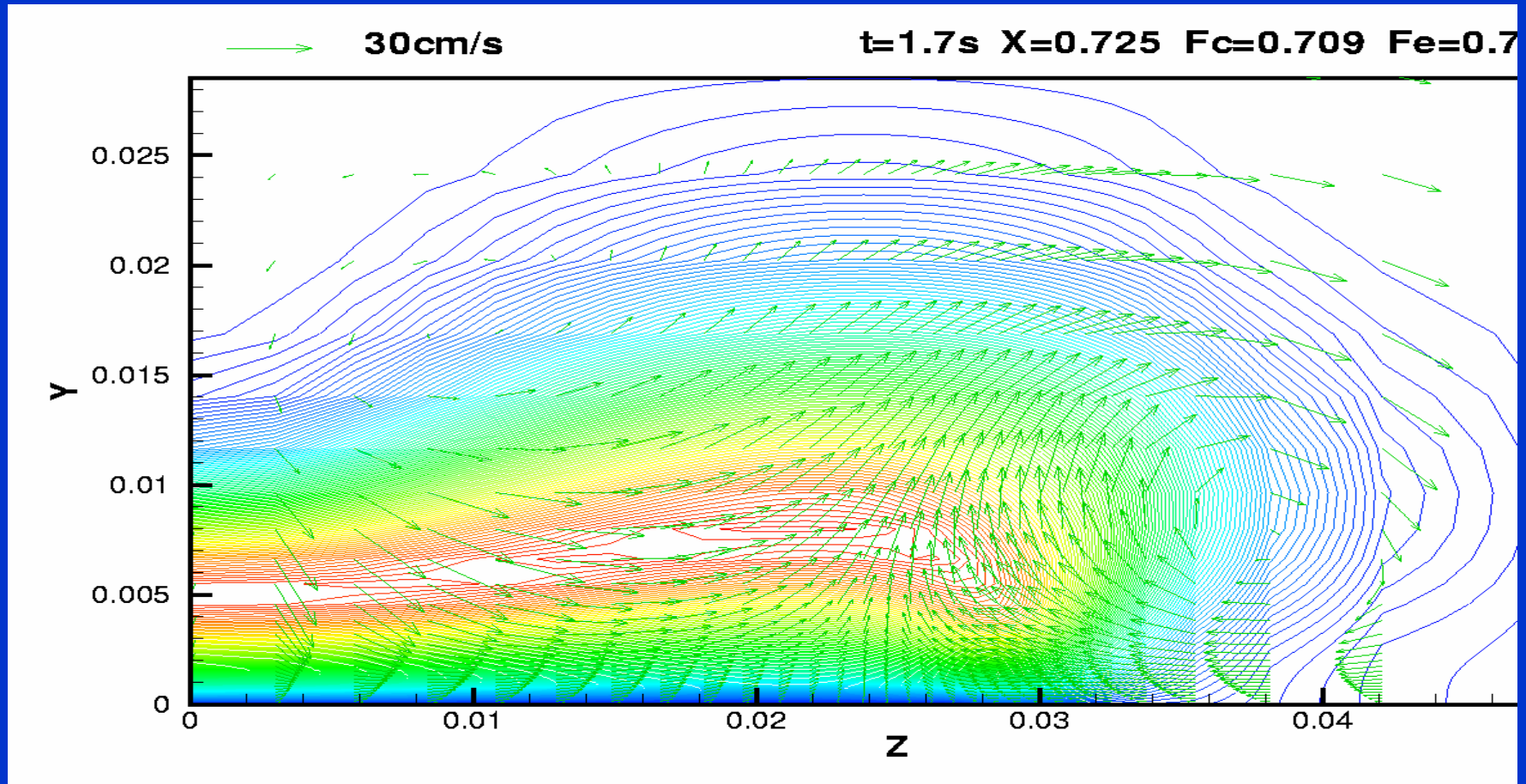
13°C, 0-g, t=1.74s, Cold Floor

# Velocity & Temperature in Symmetry Plane



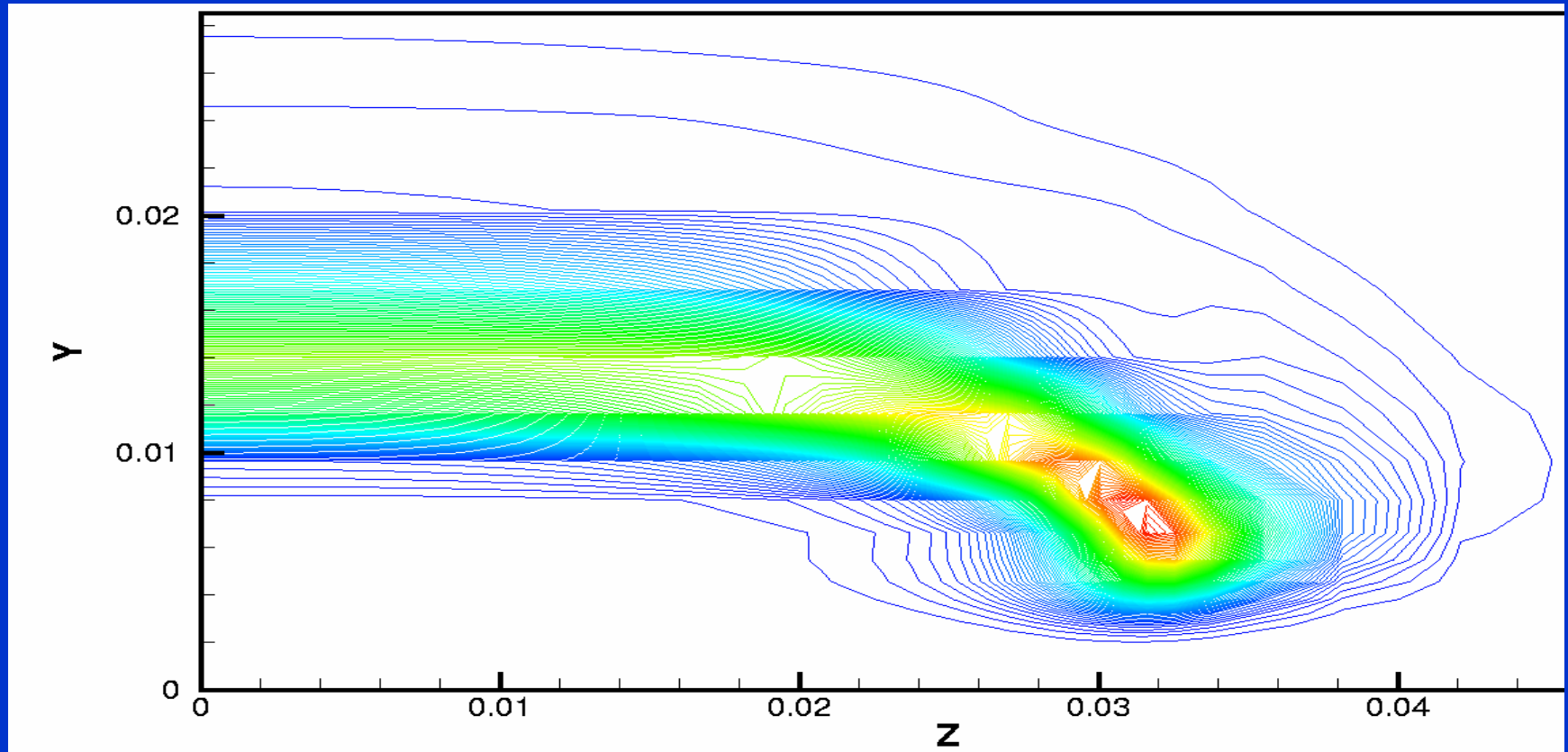
13°C, 0-g, t=1.74s. Flame remains close to surface in absence of buoyancy.

# Cross View - Velocity Vectors & Temperature Contours



13 °C, 1-g, t=1.7s, x/L=.725. Cold floor.  
Vortex on side.

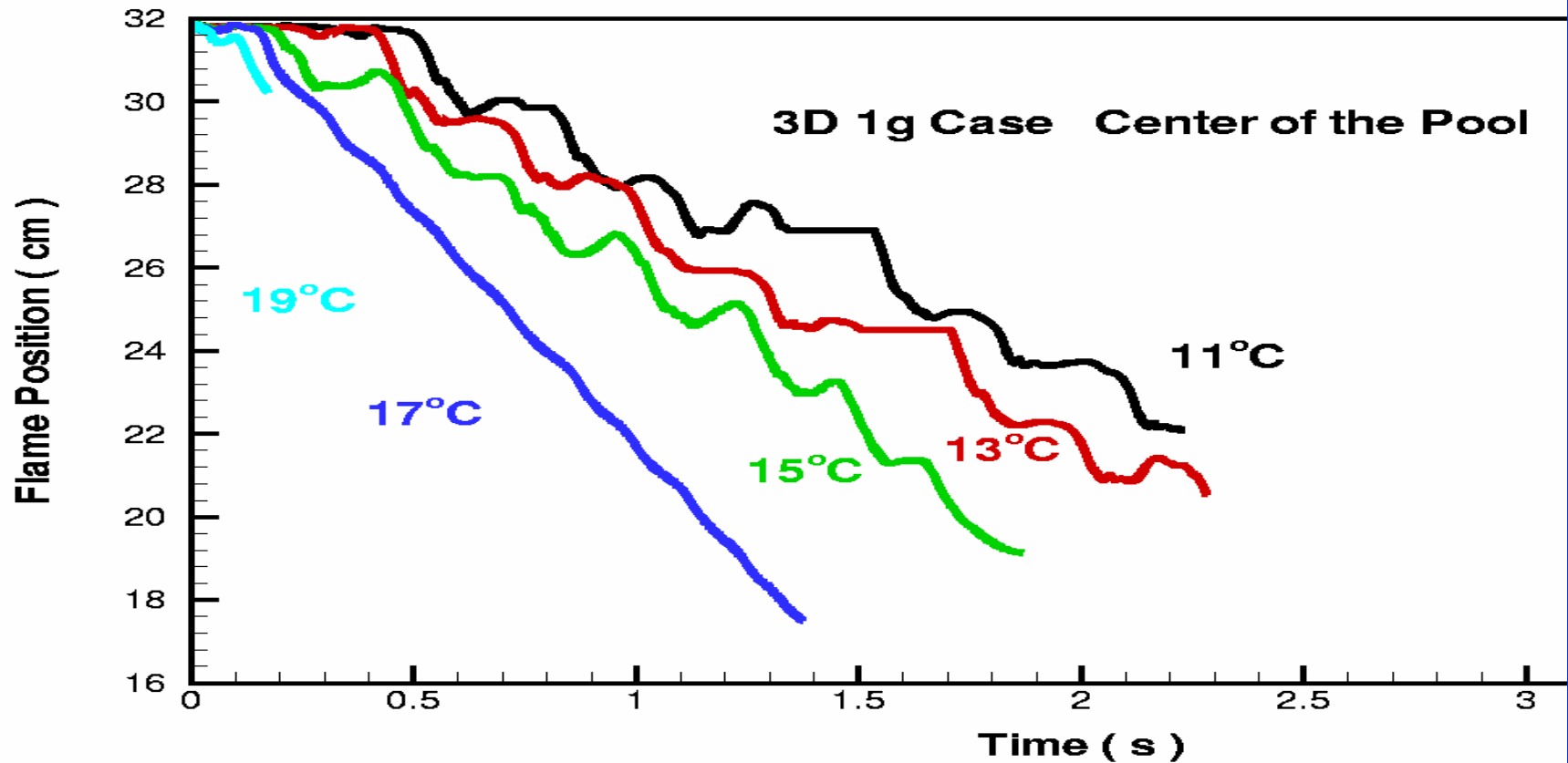
# Cross View, Behind Flame – Fuel Consumption Rate



13 °C, pulsating case, 0-g,  $t=1.74s$ ,  $x/L=.80$ .  
Cold tunnel floor.

# FLAME POSITION VS. TIME

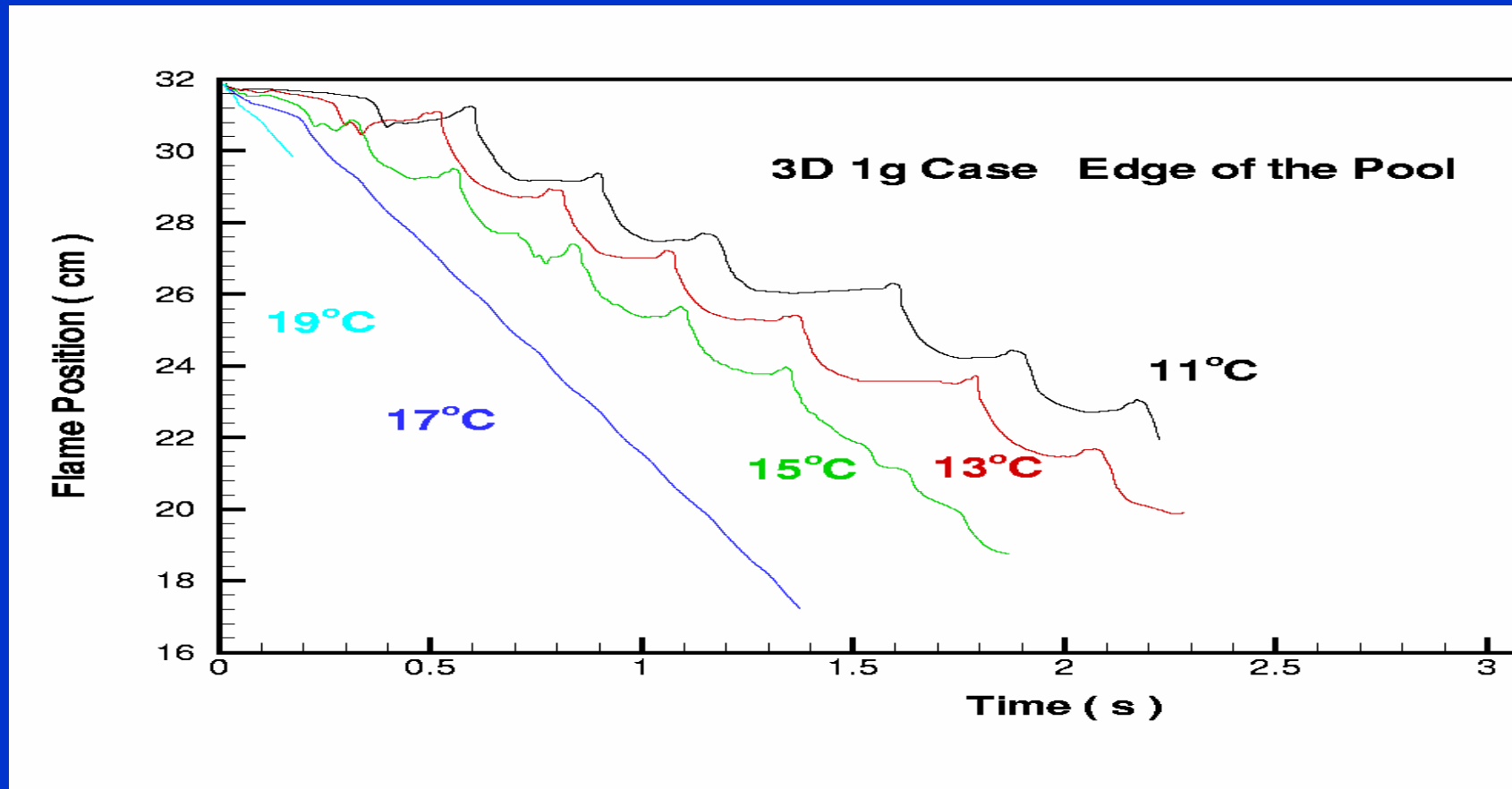
## Symmetry Plane



Hot floor, 30cm/s, 1-g, 13°C

# FLAME POSITION VS. TIME

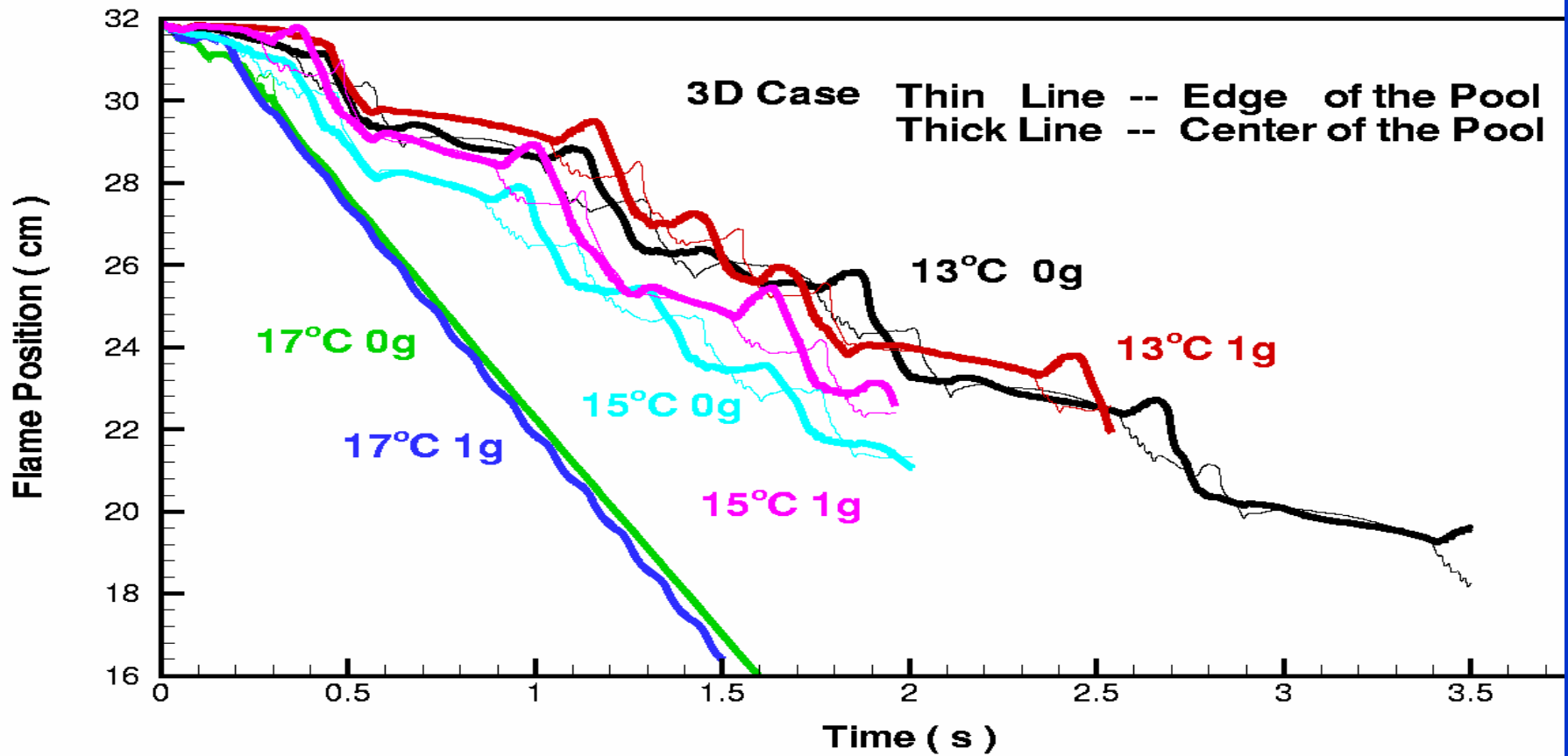
## Edge of Pool



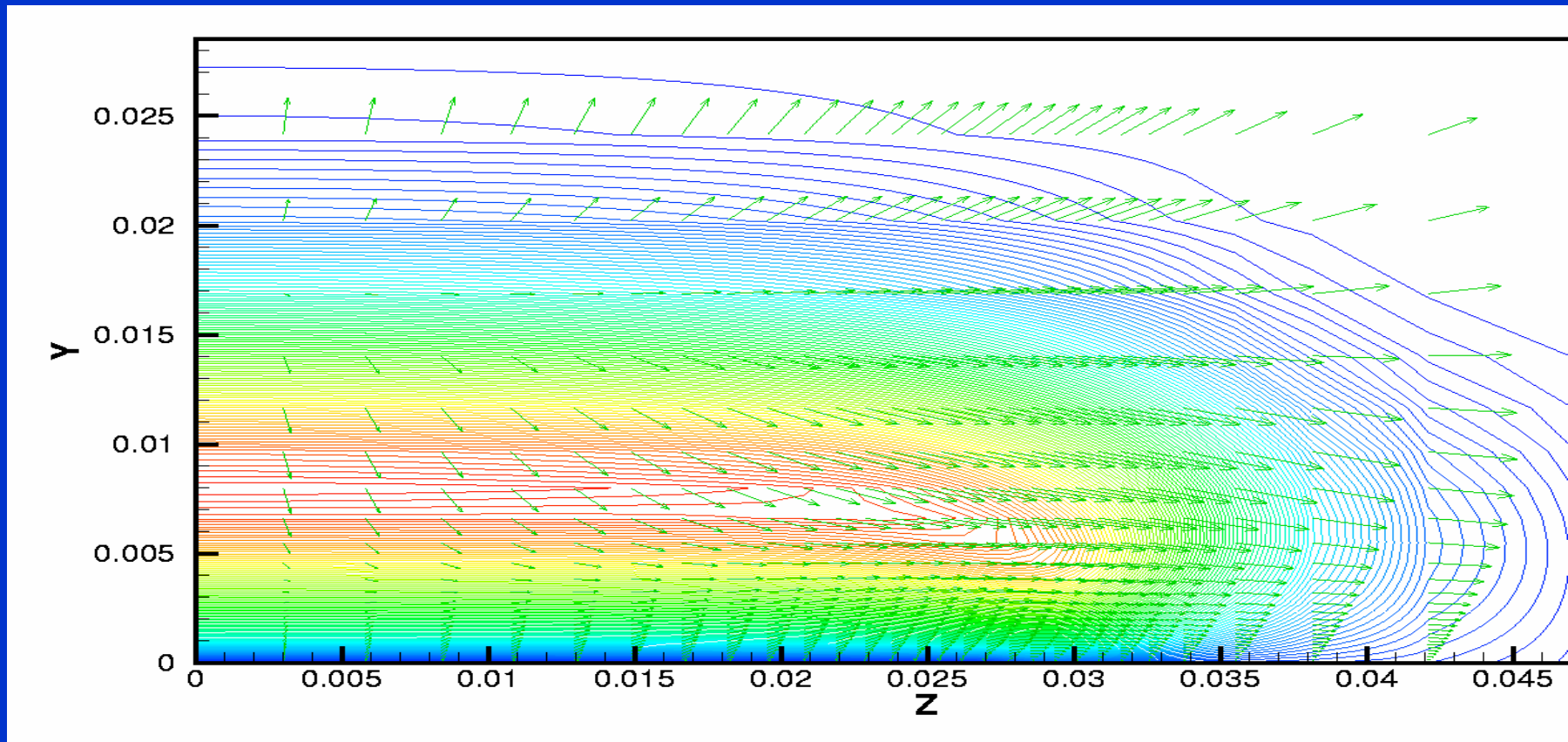
Hot floor, 30cm/s, 1-g, 13°C



# 3D 0, 1g



# Cross View - Velocity Vectors & Temperature Contours



13 °C, 0-g,  $t=1.74s$ ,  $x/L=.73$ . Cold floor.  
No vortex on side in absence of buoyancy.